



# A mammalian tripartite enhancer cluster controls hypothalamic *Pomc* expression, food intake, and body weight

Daniela Rojo<sup>a,1,2</sup> , Clara E. Hael<sup>a,1</sup>, Agustina Soria<sup>a,b</sup>, Flávio S. J. de Souza<sup>b,c</sup> , Malcolm J. Low<sup>d,3</sup> , Lucía F. Franchini<sup>a,3</sup>, and Marcelo Rubinstein<sup>a,b,d,3</sup>

Edited by John Speakman, Chinese Academy of Sciences, Shenzhen, China; received January 5, 2024; accepted March 12, 2024

Food intake and energy balance are tightly regulated by a group of hypothalamic arcuate neurons expressing the proopiomelanocortin (*POMC*) gene. In mammals, arcuate-specific *POMC* expression is driven by two *cis*-acting transcriptional enhancers known as nPE1 and nPE2. Because mutant mice lacking these two enhancers still showed hypothalamic *Pomc* mRNA, we searched for additional elements contributing to arcuate *Pomc* expression. By combining molecular evolution with reporter gene expression in transgenic zebrafish and mice, here, we identified a mammalian arcuate-specific *Pomc* enhancer that we named nPE3, carrying several binding sites also present in nPE1 and nPE2 for transcription factors known to activate neuronal *Pomc* expression, such as ISL1, NKX2.1, and ER $\alpha$ . We found that nPE3 originated in the lineage leading to placental mammals and remained under purifying selection in all mammalian orders, although it was lost in *Simiiformes* (monkeys, apes, and humans) following a unique segmental deletion event. Interestingly, ablation of nPE3 from the mouse genome led to a drastic reduction (>70%) in hypothalamic *Pomc* mRNA during development and only moderate (<33%) in adult mice. Comparison between double (nPE1 and nPE2) and triple (nPE1, nPE2, and nPE3) enhancer mutants revealed the relative contribution of nPE3 to hypothalamic *Pomc* expression and its importance in the control of food intake and adiposity in male and female mice. Altogether, these results demonstrate that nPE3 integrates a tripartite cluster of partially redundant enhancers that originated upon a triple convergent evolutionary process in mammals and that is critical for hypothalamic *Pomc* expression and body weight homeostasis.

transcriptional enhancer | transgenic mice | melanocortin | obesity | gene expression

Food intake in mammals is a highly adaptive process regulated by homeostatic mechanisms that promote the recovery of essential nutrients expended during daily activities in concert with allostatic adjustments that prepare the organism for special demands such as those involved during growth, pregnancy, and lactation (1). Instrumental in the regulation of energy balance is a group of neurons located in the arcuate nucleus of the hypothalamus that release the potent anorexigenic melanocortins  $\alpha$ -,  $\beta$ -, and  $\gamma$ -melanocyte-stimulating hormones encoded by the proopiomelanocortin gene (*POMC*). In fact, the satiety tone that melanocortins exert for most part of the day depends on high levels of hypothalamic *POMC* expression (2). The functional importance of the central melanocortin system is apparent in mice lacking *Pomc* expression specifically in arcuate neurons which develop hyperphagia and early-onset extreme obesity (3). Humans (4), mice (5), and dogs (6) with biallelic null mutations in *POMC* also develop exaggerated food intake and severe obesity.

The functional identity of arcuate melanocortin neurons is determined by a distinct set of transcription factors (TFs) including ISL1 (7), NKX2.1 (8), and PRDM12 (9). Selective ablation of each of these factors prevents the onset of *Pomc* expression and, therefore, the establishment of melanocortin neurons (7–9). The T-box factor TBX3 has also been found to play an important role in maintaining physiological levels of hypothalamic *Pomc* expression (10). In addition to this repertoire of *trans*-acting factors, arcuate *Pomc* expression in mammals depends on two evolutionary conserved *cis*-acting elements known as nPE1 and nPE2 (11, 12). These transcriptional enhancers originated from two ancient exaptation events that occurred in the lineage leading to mammals following the independent insertions of different types of retroposons into the 5' flanking region of the *POMC locus* (13, 14). Transgenic mouse assays showed that the sole presence of nPE1 or nPE2 is sufficient for arcuate-specific reporter gene expression in *POMC* neurons (11) suggesting some level of functional redundancy between these two enhancers. Moreover, genome alignments revealed that nPE1 and nPE2 are present next to each other upstream of *POMC* in all placental mammalian orders (12) indicating that they coexist under purifying selection since the radiation of mammals, around 100 mya (15–17). To investigate the adaptive value of carrying two independent hypothalamic *POMC* enhancers, instead of just one, we

## Significance

Food intake is tightly regulated by hypothalamic neurons expressing the proopiomelanocortin (*POMC*) gene. Humans, dogs, and mice carrying null mutations in *POMC* develop hyperphagia and severe obesity. Hypothalamic *POMC* expression in mammals is driven by the transcriptional enhancers nPE1 and nPE2. However, mutant mouse studies suggested that additional regulatory elements were necessary for full hypothalamic *Pomc* expression. By combining molecular evolution with reporter gene expression in transgenic zebrafish and mice, we identified nPE3, a neuronal *Pomc* enhancer present in all placental mammals except in anthropoid primates. We found that nPE3 integrates a multipartite cluster of partially redundant enhancers originated upon a unique example of triple convergent evolution. This enhancer cluster is critical for hypothalamic *Pomc* expression and body weight regulation.

Author contributions: D.R., C.E.H., F.S.J.d.S., M.J.L., L.F.F., and M.R. designed research; D.R., C.E.H., A.S., F.S.J.d.S., and L.F.F. performed research; M.J.L. and M.R. contributed new reagents/analytic tools; D.R., C.E.H., A.S., F.S.J.d.S., L.F.F., and M.R. analyzed data; and D.R. and M.R. wrote the paper.

The authors declare no competing interest.

This article is a PNAS Direct Submission.

Copyright © 2024 the Author(s). Published by PNAS. This article is distributed under Creative Commons Attribution-NonCommercial-NoDerivatives License 4.0 (CC BY-NC-ND).

<sup>1</sup>D.R. and C.E.H. contributed equally to this work.

<sup>2</sup>Present address: Department of Psychiatry and Behavioral Sciences, Stanford University School of Medicine, Palo Alto, CA 94305.

<sup>3</sup>To whom correspondence may be addressed. Email: mjlw@umich.edu, franchini.lucia@gmail.com, or mrubins@fbmc.fcen.uba.ar.

This article contains supporting information online at <https://www.pnas.org/lookup/suppl/doi:10.1073/pnas.2322692121/-DCSupplemental>.

Published April 23, 2024.

previously performed a comparative expression analysis in mutant mice carrying single and double enhancer deletions and found that E10.5 homozygous mutant embryos lacking either nPE1 or nPE2 showed great reduction (~70%) in hypothalamic *Pomc* mRNA levels, evidencing that both enhancers interact in a synergistic fashion during development (12). Similarly, adult mice also demonstrated that the concurrent presence of nPE1 and nPE2 is necessary to reach the physiological high levels of *Pomc* expression demanded to sustain normal food intake and adiposity (12). Interestingly, double homozygous mutant adults simultaneously lacking nPE1 and nPE2 were still able to express 10 to 15 % of hypothalamic *Pomc*, in contrast with arcuate POMC *knockout* mice which exhibited undetectable levels of *Pomc* mRNA in the hypothalamus at all ages (3). Together, these results suggested to us that additional partially redundant enhancers are likely to contribute to the overall expression of hypothalamic *Pomc*. Here, we combined molecular evolution and reporter gene expression studies in transgenic zebrafish and mice that led us to the identification of an arcuate specific transcriptional *Pomc* enhancer, that we named nPE3. By performing a mouse molecular genetics and metabolism approach, we also demonstrate that nPE3 integrates a tripartite enhancer cluster that is critical for hypothalamic *Pomc* expression during development and postnatal ages and assures normal food intake and body weight regulation in adult mice.

## Results

**Reporter Expression Analysis of Mammalian Conserved Elements of the *Pomc* locus in Transgenic Zebrafish.** Previous studies from our lab showed that mice lacking both, nPE1 and nPE2, still express some levels of arcuate *Pomc* mRNA (12) suggesting the existence of additional hypothalamic *Pomc* enhancers. Because functional regulatory elements tend to be under purifying selection, we searched for conserved mammalian orthologous regions within the mouse *Pomc* locus, using the PFAST software package (18) and Multiz Alignment (19) implemented through the UCSC Genome Browser (20). Within a 48 kb genomic fragment limited at its 5' and 3' ends by the adjacent genes *Dnmt3a* and *Efr3b*, respectively, we detected seven noncoding conserved sequences which have not been previously studied as potential regulatory elements (Fig. 1A and B). Two additional conserved sequences located at -28.7 and -26.1 kb have not been selected as enhancer candidates because they carry canonical CTCF binding sites and are, therefore, more likely to participate in the 3D organization of the *Pomc* locus than as transcriptional enhancers (Fig. 1A, pink columns). To test whether these seven selected sequences may act as neuronal *Pomc* enhancers, we evaluated their ability to drive EGFP expression to hypothalamic POMC neurons in transgenic zebrafish, a validated cross-species reporter expression assay we previously used when

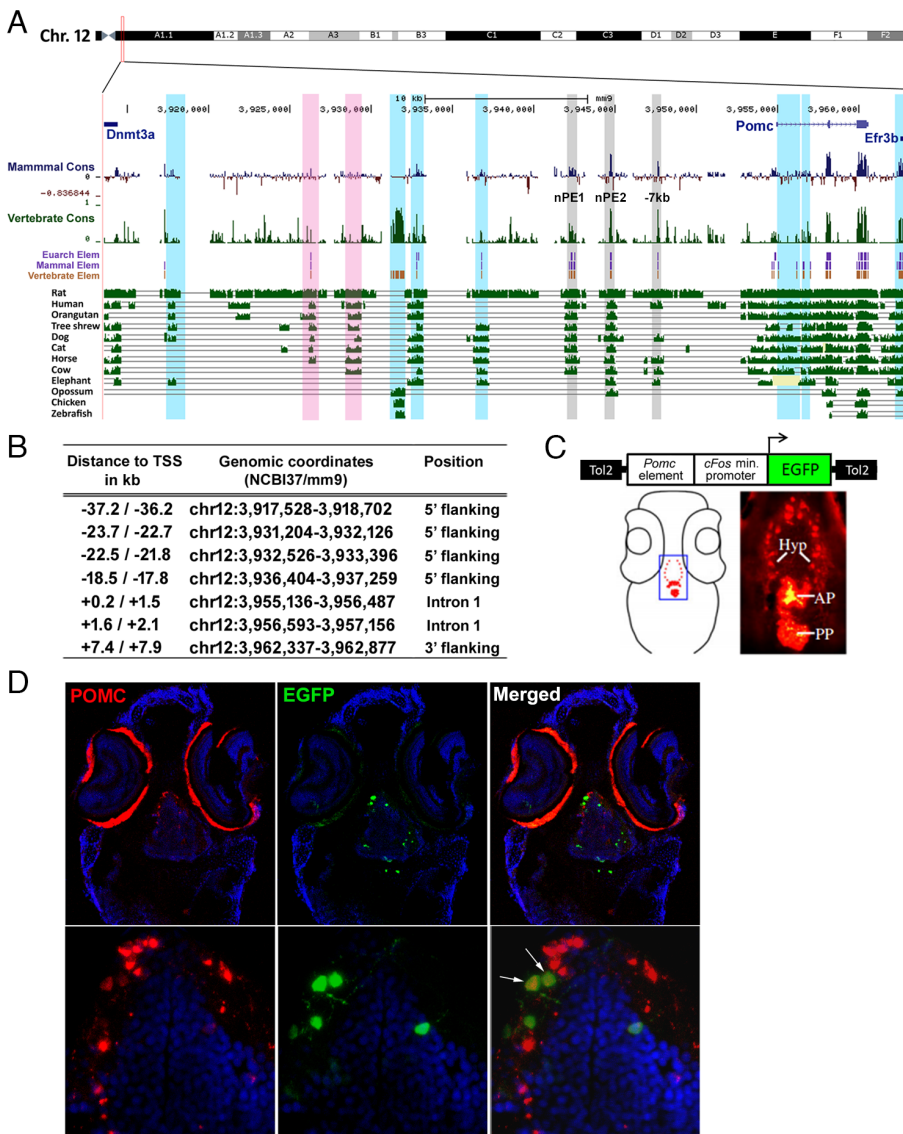


**Fig. 1.** Identification of a neuronal *Pomc* enhancer in transgenic zebrafish. (A) Custom UCSC genome browser view of local sequence alignments between regions from -40 to +8 kb of the mouse (NCBI37/mm9) and of the rat, human, orangutan, tree shrew, dog, cat, horse, cow, elephant, opossum, chicken, and zebrafish *Pomc* genes. Mammalian and vertebrate sequence conservation are shown as blue and green peaks, respectively. Vertebrate, placental mammals, and euarchontoglires conserved elements appear as colored bars (PhastCons Conserved Elements, 30-way Multiz Alignment). The three previously described *Pomc* enhancers at -12 kb (nPE1), -10 kb (nPE2), and -7 kb (pituitary enhancer) from the TSS are highlighted in gray. Two elements located at -28.7 and -26.1 kb carrying canonical CTCF binding sites are highlighted in pink. The seven conserved enhancer candidate elements selected for reporter assays in transgenic zebrafish are highlighted in light blue. (B) Location of the conserved elements in the mouse *Pomc* locus. (C) Diagram of the transgene structure based on the Tol2 system (Top), a scheme of horizontal zebrafish head cut (Bottom Left), and a previously reported immunofluorescence labeling of POMC cells (Bottom Right) taken from ref. 21. Hyp: Hypothalamus, AP: anterior pituitary gland, PP: posterior pituitary gland. (D) Representative EGFP and ACTH double immunofluorescence of transient -18 kb-cFos-*Pomc* transgenic zebrafish at 5 dpf showing reporter expression in developing hypothalamic POMC neurons.

studying nPE1 and nPE2 (21). Each of the seven transgenes (Fig. 1C) was microinjected in at least 200 zebrafish zygotes and screened for bright green fluorescence in the ventral hypothalamus of live embryos 5 d post fertilization (dpf). Selected embryos were fixed, cryostat sectioned, and analyzed by double immunofluorescence with antibodies raised against EGFP and the POMC-derived peptide ACTH. Only the conserved element located 18 kb upstream (–18 kb) of the transcriptional start site (TSS) of mouse *Pomc* was able to drive detectable EGFP expression to POMC hypothalamic neurons in transgenic zebrafish (Fig. 1D).

### The Mouse –18 kb *Pomc* Element Drives EGFP Expression to Arcuate POMC Neurons of Transgenic Mice during Development and Adulthood.

We then tested the ability of the element located at –18 kb to act as a hypothalamic *Pomc* enhancer in transgenic mice. To this end, we built a construct carrying ~700 bp of this conserved mouse element (–18.5 to –17.8 kb) upstream of a mouse *c-Fos* minimal promoter followed by EGFP coding sequences and generated three independent transgenic mouse lines. EGFP expression was then analyzed in cryosections taken from –18 kb *Pomc*-EGFP embryos, adult mouse brains, and pituitaries of the three transgenic pedigrees. Double immunofluorescence with anti-EGFP and anti-ACTH antibodies showed that the –18 kb *Pomc* element drives EGFP expression specifically to POMC neurons in E10.5, E13.5, and E15.5 transgenic mouse embryos (Fig. 2, upper rows) in the three transgenic lines (SI Appendix, Fig. S1, upper rows). Similarly, EGFP expression was detected in POMC+ hypothalamic neurons of juvenile P21 and adult P90 transgenic mice (Fig. 2, lower rows and SI Appendix, Fig. S1, lower rows) of both sexes along the entire antero-posterior, medial-lateral, and dorso-ventral axes of the arcuate nucleus (SI Appendix, Fig. S2). Quantitative coexpression of nPE3-driven EGFP in POMC neurons at all ages is indicated in SI Appendix, Table S1 for the three independent transgenic mouse lines analyzed. In contrast, EGFP expression was undetected in the developing or adult pituitary, an endocrine tissue where *Pomc* is also expressed at great levels (Fig. 2). Together, these results indicate that the conserved sequences located between –18.5 to –17.8 kb from the *Pomc* TSS act as a specific neuronal *Pomc* hypothalamic enhancer during development and postnatal stages. Based on its functional similarity with nPE1 and nPE2, we named this element nPE3 (neuronal *Pomc* enhancer 3).

**Molecular Evolution of nPE3.** To investigate the evolutionary origin of nPE3, we searched for paralog sequences present in available vertebrate genomes using BLAT (20) and BLAST (22) tools. We found that nPE3 is a conserved sequence present in all placental mammalian orders but absent from marsupials, monotremes, and all other vertebrate classes (Fig. 3A). Using the sequence alignment algorithms ClustalW2 (23) and Blast2seq (24) we also found that nPE3 sequences are unrelated to those of nPE1 and nPE2 ruling out the possibility of a duplication origin. In addition, nPE3 sequences did not show similarity with the retrotransposon elements that gave rise to nPE1 (14) or nPE2 (13). To identify possible exaptation events from other ancient transposable elements (TE), we searched for nPE3 paralogs in the genomes of representative species of several mammalian orders including Rodentia (*Mus musculus*), Carnivora (*Canis familiaris*), Artiodactyla (*Bos taurus*), Xenarthra (*Dasyus novemcinctus*), Proboscidea (*Loxodonta africana*), Cetacea (*Tursiops truncatus*), Insectivora (*Echinops telfairi*), Chiroptera (*Pteropus vampyrus*), and Lagomorpha (*Oryctolagus cuniculus*), using Blastn (<https://blast.ncbi.nlm.nih.gov/Blast.cgi>) and 639 bp of mouse nPE3 as a query (mm10; chr12:3,936,524 to 3,937,162). Our results indicated that the most significant hits in all species correspond

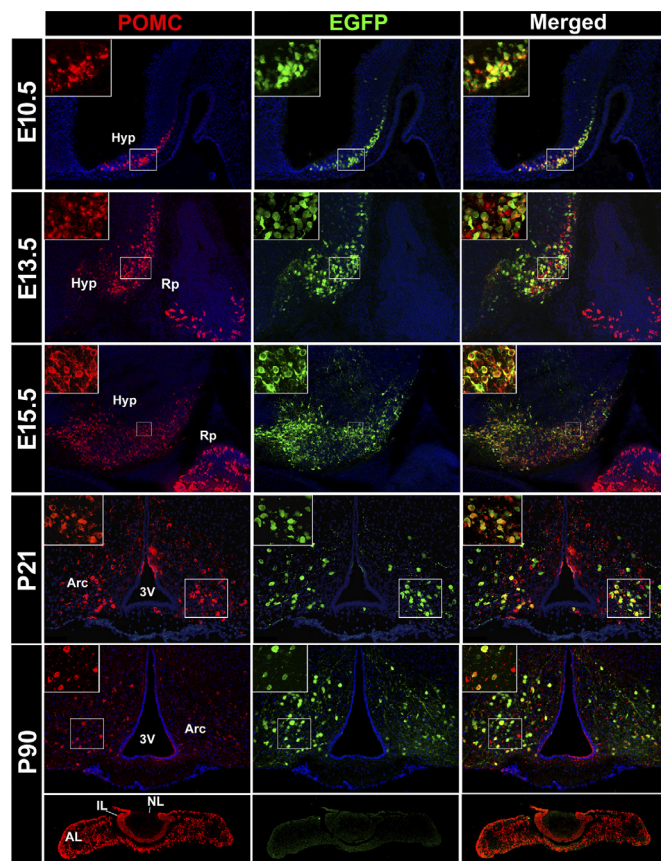


**Fig. 2.** The –18 kb mouse *Pomc* element drives EGFP expression to developing and adult mouse hypothalamic POMC neurons. Reporter gene expression analysis in sagittal cryosections at the level of the developing hypothalamus of –18 kb *Pomc*-EGFP transgenic mouse embryos collected at E10.5, E13.5, and E15.5, and in coronal cryosections at the level of the arcuate nucleus of P21 and P90 mice. *Insets* are magnified views of confocal images showing that EGFP+ cells (green) coexpress POMC (red). Hyp, mediobasal hypothalamic area; Rp, Rathke's pouch; Arc, arcuate nucleus of the hypothalamus; 3V, third ventricle; AL, anterior lobe; IL, intermediate lobe; NL, neural lobe of the pituitary gland.

to the nPE3 orthologues. A second significant hit spanning mouse nPE3 nucleotides 490 to 550 displayed high identity with Lx2B2 LINE1-derived sequences found in several regions of most mammalian genomes analyzed. Other mouse nPE3 regions showed significant identity with sequences derived from different TE families scattered in the mouse genome. For example, nucleotides 109 to 210 matched with Lx2 LINE1-derived sequences; nucleotides 137 to 217 matched with Alu SINE-derived sequences and nucleotides 404 to 502 appear to derive from a MIR1b SINE (Fig. 3A). Thus, our results show that nPE3 has been built throughout evolution as a patchwork of unrelated sequences (Fig. 3A). Hence, the three mammalian hypothalamic *POMC* enhancers have a distinct and independent evolutionary origin.

A salient feature observed in Fig. 3A, is the absence of conserved nPE3 sequences in the human genome. Further phylogenetic footprinting analysis using MultiPipMaker (25) and the mouse genome as a reference showed that nPE3 is present in all groups of placental mammals including Primates of the Strepsirrhini clade (e.g., lemurs and galagos) and the tarsier *Carlito syrichta* (Fig. 3B), but absent from the *POMC* loci of monkeys, apes, and humans (Fig. 3B), suggesting a specific loss of this enhancer in the Simiiformes clade. To evaluate the magnitude of the deletion that led to the loss of nPE3 in an ancestor of Simiiformes, we performed a MultiPipMaker analysis of 21 kb around nPE3 using the tarsier *locus* as reference and looked for the presence of unambiguously aligned regions,

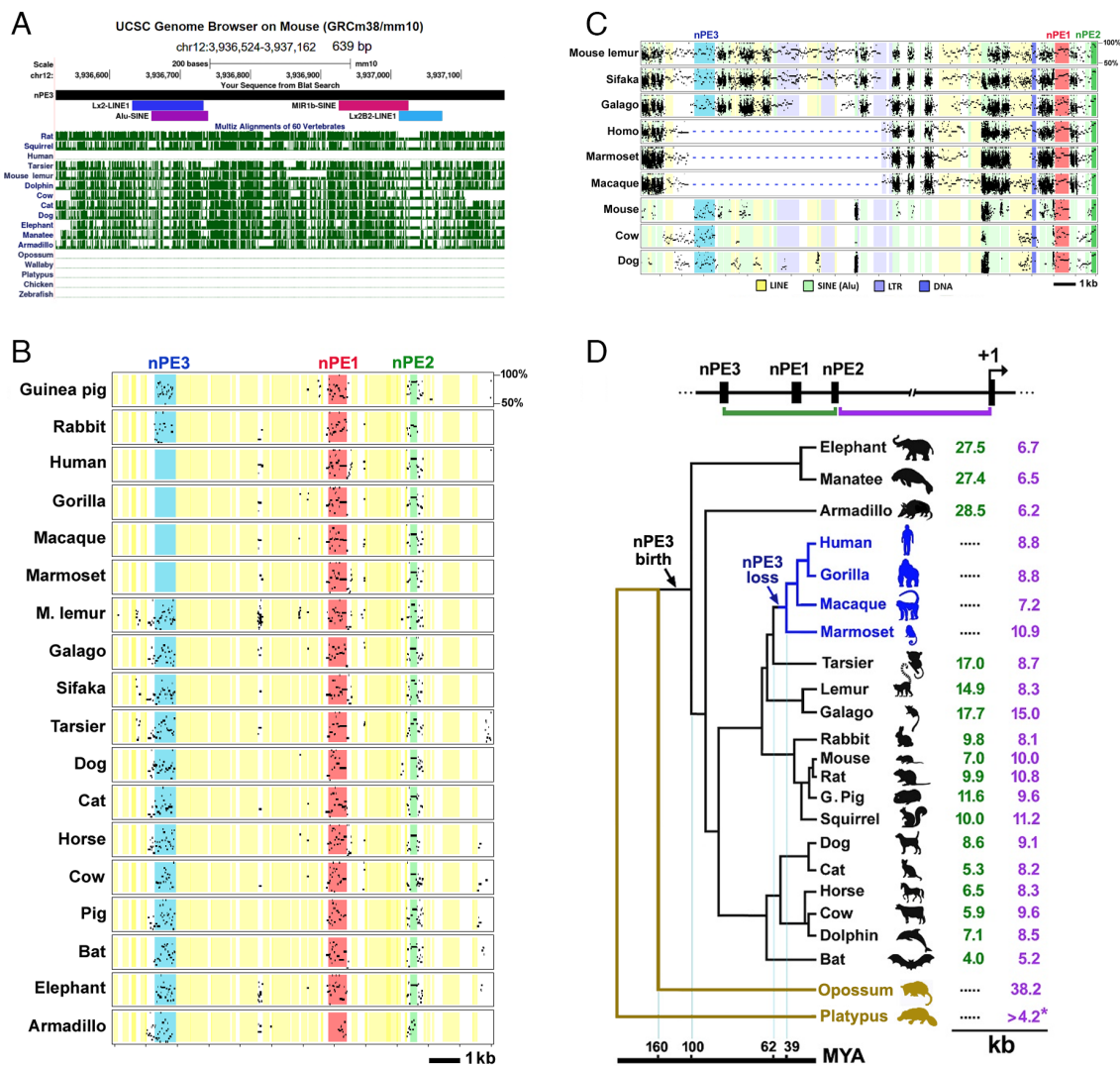


**Fig. 3.** Molecular evolution of nPE3. (A) Custom UCSC Genome Browser view of 639 bp of mouse nPE3 sequence (mm10; chr12:3,936,524 to 3,937,162). Transposable element sequences showing identity with mouse nPE3 found by Blastn are depicted with different colors. Multiz alignment of 60 Vertebrates shows that nPE3 is highly conserved (green peaks) in all placental mammalian orders. (B) MultiPipMaker phylogenetic comparison of the 5' region of mouse *Pomc* (*Mus musculus*) shows that different from nPE1 and nPE2 which are present in all Eutherian species, nPE3 is absent from Simiiformes such as the marmoset (*Callithrix jacchus*), macaque (*Macaca mulatta*), gorilla (*Gorilla gorilla*), and humans (*Homo sapiens*). (C) Comparison of the *POMC* locus of various mammals using the tarsier *Carolito syrichta* as a reference genome. MultiPipMaker aligned sequences and derived from mobile elements of LINE (yellow), SINE-Alu (green), LTR (purple), or DNA (blue) families are indicated (Bottom). Lost segments carrying nPE3 in Simiiformes are indicated with dot lines. (D) The drawing represents the phylogeny of all placental mammalian orders, and marsupials and monotremes as outgroups. nPE3 (black arrow) appeared before the radiation of all placental mammals and was lost (blue arrow) after the tarsier/Simiiformes split and before the Catarrhini/Platyrrhini split. The distance (kb) of the nPE3-nPE1-nPE2 enhancer cluster is indicated in green and the distance from nPE2 to the TSS in purple.

including ancient repetitive elements, between tarsier and other primates and nonprimate mammals (Fig. 3C). We found that the tarsier sequence that spans from 2 kb upstream of nPE3 until nPE1 aligns well with orthologous regions of other primates like the mouse lemur (*Microcebus murinus*) and Coquerel's sifaka (*Propithecus coquereli*) (Fig. 3C) and, to a lesser extent, to those of mouse, cattle and dog. In contrast, the alignment with the equivalent regions of *Homo sapiens*, marmoset (*Callithrix jacchus*), and macaque (*Macaca mulatta*) is interrupted ~500 bp upstream of nPE3 until ~8 kb downstream of tarsier nPE3, within the remnants of an ancient LTR retroposon (MaLR; Fig. 3C). Thus, the deletion that caused the loss of nPE3 is much larger than the enhancer itself. Altogether, our results indicate that nPE3 got fixed in the *POMC* locus after the Metatheria/Eutheria split (~160 mya) and before the radiation of placental mammals (~100 mya) by an independent evolutionary event and since then remained as a conserved sequence

in all placental mammalian orders (Fig. 3B–D). However, a DNA segment of ~8.5 kb encompassing nPE3 underwent a lineage-specific deletion sometime between the Tarsier/Simiiformes split (~62 mya) and the Catarrhini (Old World primates)/Platyrrhini (New World primates) split (~39 mya) (26) (Fig. 3C and D). The distance between nPE3 and nPE1 shows some variability in mammals (Fig. 3D). In the genome of the nine-banded armadillo (*D. novemcinctus*; supraorder Xenarthra), nPE3 is ~28 kb upstream of nPE1, whereas in species from the Afrotheria order such as the African elephant (*L. africana*) and the Amazonian manatee (*Trichechus inunguis*), the distance between both enhancers is ~26 kb. In primates like lemurs and tarsiers, both enhancers are in closer proximity (13 to 16 kb), and even closer in some rodents and bats (less than 5 kb), showing that the loss and gain of DNA in the neighborhood of *POMC* regulatory regions has been a common feature in mammalian evolution (Fig. 3D).

**TF Binding Sites Present in nPE3.** Analysis of mouse nPE3 sequences using JASPAR (27) detected several canonical binding sites for TFs of different families. Some of these TFs are known to participate in arcuate-specific and hormonal regulation of *Pomc* expression, including ISL1 (7), NKX2.1 (8), ER $\alpha$  (28), TBX3 (10), and PRDM12 (9) (Fig. 4A). Other detected TF binding sites (TFBS) families including SOX and Nuclear Receptors (NR) match with cognate TFs present in the arcuate POMC neuron transcriptome such as *Sox1*, *2*, *3* and *14*, *Nr0b1*, and *Nr5a1* (29). Some of these binding sites are located in most conserved sequences, as indicated by the presence of PhastCons regions (Fig. 4A). A ClustalW2 alignment of several mammalian genomes using the largest PhastCon of nPE3 together with its immediate upstream region (red box in Fig. 4A) followed by JASPAR analysis is depicted in Fig. 4B in larger detail. Chromatin immunoprecipitation (ChIP) assays using chromatin harvested from adult male hypothalami and antibodies for ISL1, NKX2.1, SOX2, or ER $\alpha$  showed that these TFs bind to nPE3 sequence in vivo (Fig. 4C). Identical results were found when using the anti-ER $\alpha$  antibody and hypothalamic chromatin from adult females (Fig. 4C). By performing multiple double immunofluorescence in sections from E10.5 (Top) and adult (Bottom) nPE3-EGFP transgenic mice, we found that nPE3 drives EGFP expression to developing and adult arcuate neurons expressing ISL1, NKX2.1, and SOX2 (SI Appendix, Fig. S3, Upper rows). In addition, we found that EGFP and ER $\alpha$  are coexpressed in ~50% of nPE3-EGFP arcuate neurons of females and males (SI Appendix, Fig. S3, Bottom row).

Although nPE1, nPE2, and nPE3 have distinct evolutionary origins, each of them drives reporter gene expression specifically to arcuate POMC neurons in transgenic mice (14) and Fig. 2, suggesting that the 3 neuronal *Pomc* enhancers share a common array of canonical binding sites for TFs known to activate arcuate *Pomc* expression. Using the JASPAR database, we analyzed nPE1, nPE2, and nPE3 sequences and collected all significant hits ( $P < 0.049$ ) for canonical TFBS. We further processed this dataset to identify TFBS that are present in the 3 nPE sequences (Dataset S1)

and found that, indeed, nPE1, nPE2, and nPE3 share canonical motifs for STAT3, NKX2.1, ISL1, and for TFs of the SOX, ER, and NR families (SI Appendix, Fig. S4 B–E). These results suggest that although having unrelated evolutionary origins, the 3 neuronal *Pomc* enhancers share a common transcriptional code (SI Appendix, Fig. S4E) that likely determines the identity of hypothalamic melanocortin neurons during development and maintains arcuate-specific *Pomc* expression in postnatal life.

**Critical Role of nPE3 in Hypothalamic *Pomc* Expression during Development.** To evaluate the functional relevance of nPE3 in hypothalamic *Pomc* expression at different developmental and postnatal stages, we deleted nPE3 from the mouse genome by targeting Cas9 endonuclease to the 5' and 3'-ends of nPE3 using two sgRNAs microinjected into C57BL/6J zygotes (SI Appendix, Fig. S5). F1 mice carrying a 629 bp deletion encompassing nPE3 sequences were used to establish a colony of *Pomc*<sup>+ΔnPE3</sup> breeders that yielded homozygous *Pomc*<sup>ΔnPE3/ΔnPE3</sup> mutants (Δ3/Δ3), heterozygous *Pomc*<sup>+ΔnPE3</sup> (+/Δ3) and *Pomc*<sup>+/+</sup> littermates in Mendelian ratios. We determined *Pomc* mRNA levels at the onset of hypothalamic *Pomc* expression in E10.5 embryo heads of both sexes by quantitative RT-PCR and found greatly reduced levels of *Pomc* mRNA in homozygous Δ3/Δ3 E10.5 female embryos, reaching only 20.4 ± 3.3 % relative to the levels detected in their *wild-type* sisters (Fig. 5A). Hypothalamic *Pomc* expression was also greatly reduced in Δ3/Δ3 E10.5 male embryos which showed 28.0 ± 6.3 % of *Pomc* mRNA levels relative to those found in their *wild-type* brothers (Fig. 5B). E10.5 heterozygous +/Δ3 embryos showed intermediate levels of *Pomc* mRNA in both sexes compared to their *wild-type* *Pomc*<sup>+/+</sup> siblings: 53.6 ± 11.0 % and 83.9 ± 10.3 % for females and males, respectively (Fig. 5 A and B). E12.5 Δ3/Δ3 embryos of both sexes also showed a great reduction in hypothalamic *Pomc* expression compared with their *wild-type* siblings, as detected by ACTH immunofluorescence in sagittal sections (Fig. 5 C and D and SI Appendix, Figs. S6 and S7). Together, these results indicate that nPE3 plays a major role in

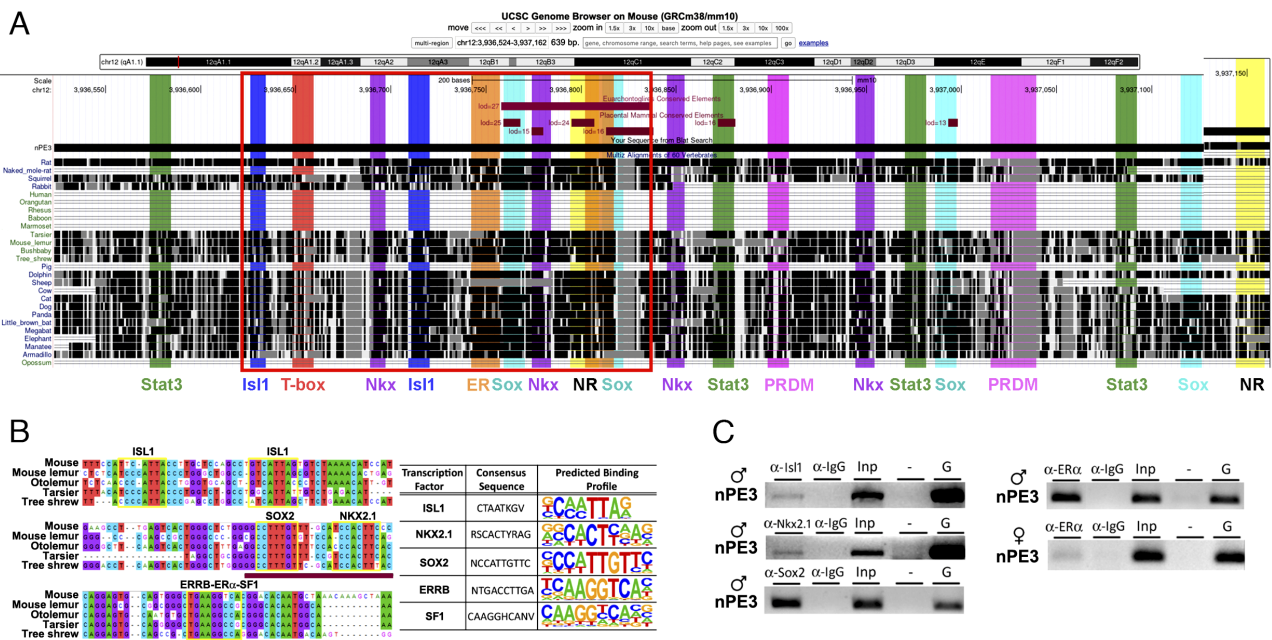


**Fig. 4.** TFBS present in nPE3. (A) Custom UCSC Genome Browser view of 639 bp of mouse nPE3 sequence (mm10; chr12:3,936,524 to 3,937,162). TFBS identified using JASPAR are indicated with a code color, some of which are present in most conserved sequences, as indicated by the Euarcontoglines and placental mammals Phastcons elements (dark red horizontal bars). (B) A ClustalW2 alignment using the largest PhastCon of nPE3 together with its immediate upstream region (red box in A) followed by JASPAR analysis is depicted in further detail. Nucleotides corresponding to the Phastcons are underlined. Canonical motifs for TFBS are indicated (Right). (C) ChIP assay with adult mice hypothalamic chromatin for testing in vivo binding of ISL1, NKX2.1, SOX2, and ER $\alpha$  to nPE3 sequence.

assembling the transcriptional machinery leading to the early developmental onset of neuronal *Pomc* expression.

**Contribution of nPE3 to Hypothalamic *Pomc* Expression in Adult Mice.** We then evaluated hypothalamic *Pomc* mRNA levels in 20-wk-old adult mice and found that  $\Delta 3/\Delta 3$  mutant males expressed  $66.9 \pm 11.5\%$  of *Pomc* relative to their *wild-type* siblings (WT,  $n = 7$ ; KO,  $n = 9$ ; Student's *t* test:  $t = 1.91$ ,  $df = 14$ ,  $P < 0.05$ ) (Fig. 5F) whereas hypothalamic *Pomc* mRNA levels in 20-wk-old  $\Delta 3/\Delta 3$  females were  $76.6 \pm 10.6\%$  relative to their *wild-type* littermates, a difference that did not reach statistical significance (WT,  $n = 8$ ; KO,  $n = 7$ ; Student's *t* test:  $t = 1.58$ ,  $df = 13$ ,  $P = 0.07$ ) (Fig. 5E). This level of reduction of *Pomc* expression observed in homozygous  $\Delta 3/\Delta 3$  mutants did not impair body weight regulation or adiposity, as observed in mice fed ad libitum with regular chow for their first 20 wk of age (Fig. 5G). Altogether, the relative contribution of nPE3 showed to be maximal at the onset of hypothalamic *Pomc* expression and more limited in adult mice, probably because of partial redundancy with nPE1 and nPE2.

**Multiple Ablation of Neuronal *Pomc* Enhancers from the Mouse Genome.** To gain further insight into the specific contribution of nPE3 to neuronal *Pomc* expression at different developmental stages, we sought to compare hypothalamic *Pomc* mRNA levels present in triple mutant mice deficient in nPE1, nPE2, and nPE3 with those present in double mutants carrying only nPE3 but lacking nPE1 and nPE2. To this end, we used the same CRISPR/Cas9 approach to target nPE3 into C57BL/6J zygotes carrying *Pomc* <sup>$\Delta nPE1, \Delta nPE2$</sup>  alleles and obtained a colony of heterozygous *Pomc* <sup>$\Delta nPE1, \Delta nPE2, \Delta nPE3$</sup>  mice ( $\Delta 1\Delta 2\Delta 3$ ) that were bred to generate homozygous nPE1, nPE2, and nPE3 triple mutants ( $\Delta 1\Delta 2\Delta 3/\Delta 1\Delta 2\Delta 3$ ) and their *wild-type* *Pomc*<sup>+/+</sup> littermates. In addition, we crossed heterozygous nPE1 and nPE2 double mutants ( $\Delta 1\Delta 2$ ) to generate homozygous  $\Delta 1\Delta 2/\Delta 1\Delta 2$  mutants and their *wild-type*

*Pomc*<sup>+/+</sup> littermates, also in a C57BL/6J background (12). A qRT-PCR study performed with mRNA taken from heads of E11.5 embryos showed almost undetectable levels of *Pomc* expression in double  $\Delta 1\Delta 2/\Delta 1\Delta 2$  ( $1.6 \pm 0.2\%$ ) and triple  $\Delta 1\Delta 2\Delta 3/\Delta 1\Delta 2\Delta 3$  ( $2.1 \pm 0.4\%$ ) homozygous enhancer mutants relative to their *wild-type* littermate levels (Fig. 6A). A similar result was found by immunofluorescence in sagittal sections of E12.5 embryos (Fig. 6B and E, Top row), an age that marks the peak of neurogenesis for POMC neurons (30). At this developmental stage, the number of POMC+ neurons and their signal intensity in the developing hypothalamus were drastically reduced in homozygous  $\Delta 1\Delta 2/\Delta 1\Delta 2$  (Fig. 6B and E, Top Center panel) and even lower in homozygous  $\Delta 1\Delta 2\Delta 3/\Delta 1\Delta 2\Delta 3$  (Fig. 6B and E, Top Right panel) in comparison with *wild-type* E12.5 embryos (Fig. 6B and E, Top Left panel) (SI Appendix, Fig. S8). The relative contribution of nPE3 to neuronal *Pomc* expression became further apparent at E15.5, a developmental stage in which hypothalamic *Pomc* mRNA levels were also significantly more affected in triple  $\Delta 1\Delta 2\Delta 3/\Delta 1\Delta 2\Delta 3$  than in double  $\Delta 1\Delta 2/\Delta 1\Delta 2$  homozygous mutants relative to WT E15.5 embryos (Fig. 6C,  $P = 0.037$  and Fig. 6E, center row panels). The relative contribution of nPE3 to hypothalamic *Pomc* expression was even greater at P0, a time-point in which  $\Delta 1\Delta 2/\Delta 1\Delta 2$  mutants displayed many more and brighter hypothalamic POMC+ neurons than  $\Delta 1\Delta 2\Delta 3/\Delta 1\Delta 2\Delta 3$  triple mutants which showed negligible levels of immunofluorescence (Fig. 6D,  $P = 0.002$ ; Fig. 6E, lower row; and SI Appendix, Fig. S8). Thus, despite the fact that nPE3 by itself was able to drive reporter gene expression to arcuate POMC neurons in transgenic mice (Fig. 2) and that  $\Delta 3/\Delta 3$  embryos showed greatly reduced hypothalamic *Pomc* expression (Fig. 5A and B), the sole presence of nPE3 in  $\Delta 1\Delta 2/\Delta 1\Delta 2$  mutants was only partially able to compensate for the absence of nPE1 and nPE2 from the arcuate *Pomc* enhancer cluster that sustains normal *Pomc* expression levels during development.

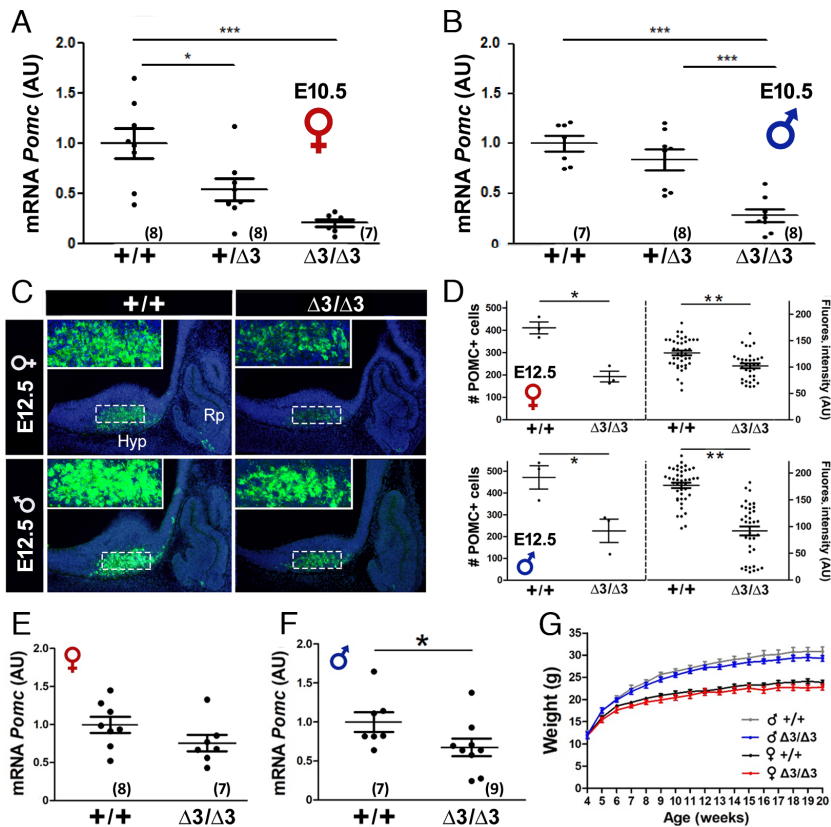


**Fig. 5.** nPE3 is critical for *Pomc* expression in the developing hypothalamus (A–D). (A and B) qRT-PCR of *Pomc* mRNA from heads of E10.5 *wild-type* (+/+), heterozygous +/ $\Delta 3$  and homozygous  $\Delta 3/\Delta 3$  littermate female (A) and male (B) embryos. Values were normalized to  $\beta$ -actin mRNA and expressed in arbitrary units (AU). *n* per group is indicated between parentheses. Data indicate the mean  $\pm$  SEM. One-way ANOVA ( $F = 12.19$  for females and  $F = 20.24$  for males) followed by Tukey's post hoc test  $*P < 0.01$ ,  $***P < 0.001$ . Hyp, mediobasal hypothalamus; Rp, Rathke's pouch. (C) Immunofluorescence using an anti-ACTH antibody (green) in sagittal cryosections of representative E12.5 *wild-type* (+/+) and  $\Delta 3/\Delta 3$  littermate female (Top) and male (Bottom) embryos. Insets are confocal magnified views of the indicated boxes. (D) Quantification of POMC+ hypothalamic cells (Left) and their fluorescence intensity (Right) measured in three cryosections of E12.5 female (Top) and male (Bottom) embryos ( $n = 3$ ). Data represent the mean  $\pm$  SEM. One-tailed Mann-Whitney test and one-tailed Student's *t* test  $*P < 0.05$ ,  $***P < 0.001$ . Importance of nPE3 in hypothalamic *Pomc* expression in adult mice. (E and F) qRT-PCR of *Pomc* mRNA from the hypothalamus of *wild-type* (+/+) and homozygous  $\Delta 3/\Delta 3$  20-wk-old females (E) and males (F). Values were normalized to  $\beta$ -actin mRNA and expressed in AU. *n* per group is indicated between parentheses. Data represent the mean  $\pm$  SEM. One-tailed Student's *t* test  $*P < 0.05$ . (G) Body weight curves for *wild-type* (+/+) and  $\Delta 3/\Delta 3$  20-wk-old females and males. Data represent the mean  $\pm$  SEM. No statistically significant differences were observed.

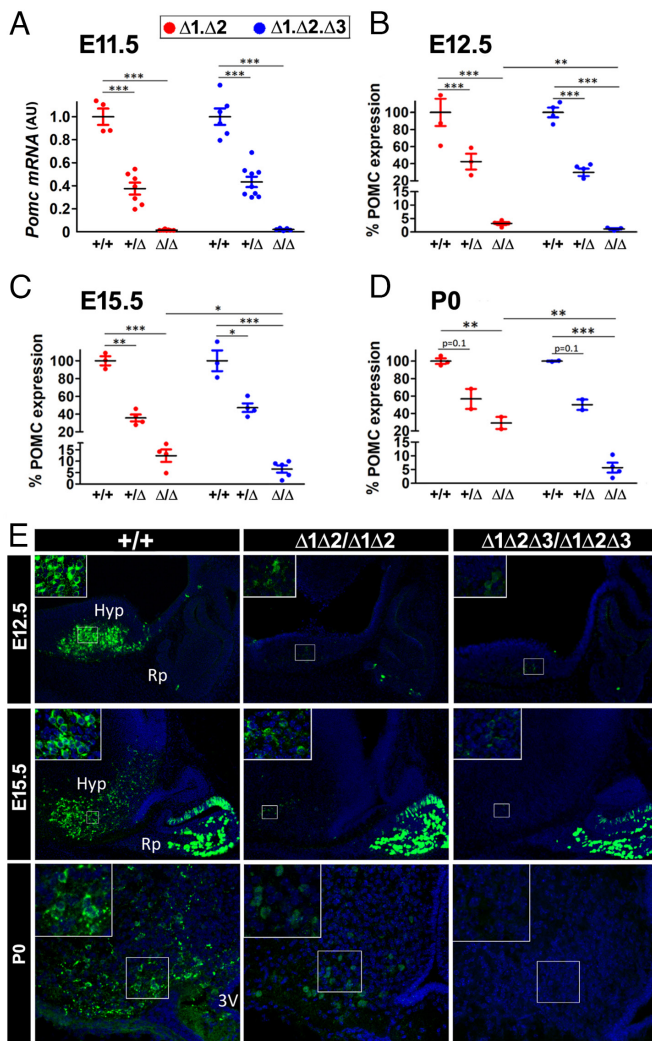


**Fig. 6.** Relative contribution of nPE3 to hypothalamic *Pomc* expression during development. (A) qRT-PCR of *Pomc* mRNA obtained from heads of *wild-type* (+/+), heterozygous *Pomc*<sup>Δ1Δ2</sup> or *Pomc*<sup>Δ1Δ2Δ3</sup> (+/Δ), and homozygous *Pomc*<sup>Δ1Δ2/Δ1Δ2</sup> or *Pomc*<sup>Δ1Δ2Δ3/Δ1Δ2Δ3</sup> (Δ/Δ) E11.5 littermate embryos. RNA was normalized to  $\beta$ -actin mRNA and expressed in AU. At least  $n = 4$  per group. (B–D) POMC expression represents the product of the mean integrated immunofluorescence density of positive cells and the number of POMC+ cells compared to controls in three cryosections of the developing hypothalamus of E12.5, E15.5, and P0 mice ( $n = 3$  to 5). (E) Representative immunofluorescence using an anti-ACTH antibody (green) in sagittal cryosections of *wild-type* (+/+), *Pomc*<sup>Δ1Δ2/Δ1Δ2</sup> (Δ1Δ2/Δ1Δ2) and *Pomc*<sup>Δ1Δ2Δ3/Δ1Δ2Δ3</sup> (Δ1Δ2Δ3/Δ1Δ2Δ3) E12.5, E15.5, and P0 mice. Insets are confocal magnified views of the indicated boxes. Hyp, mediobasal hypothalamic area; Rp, Rathke's pouch area; 3V, third ventricle. Data represent the mean  $\pm$  SEM compared by two-way ANOVA. \* $P < 0.05$ , \*\* $P < 0.01$ , \*\*\* $P < 0.001$ . Two-way ANOVA, followed by the Holm–Sidak post hoc test.

**Effects of the Multiple Lack of Neuronal *Pomc* Enhancers in Adult Mice.** Similar to what we observed during development, hypothalamic *Pomc* mRNA levels assessed by qRT-PCR in 16-wk-old double and triple homozygous enhancer mutant mice were also greatly impaired in comparison to those detected in their *wild-type* littermates, with slightly lower *Pomc* mRNA in Δ1Δ2Δ3/Δ1Δ2Δ3 than in Δ1Δ2/Δ1Δ2 mice, a difference that reached statistical significance only in females (Fig. 7A). Similar results were found by performing quantitative POMC immunofluorescence on coronal hypothalamic sections (Fig. 7B and C). In Δ1Δ2Δ3/Δ1Δ2Δ3 triple mutants of both sexes, POMC+ neurons were nearly undetectable (Fig. 7B and C). These differential features were observed all along the hypothalamic antero-posterior axis (SI Appendix, Fig. S9). Double and triple heterozygous female and male mutant adults displayed similar intermediate levels of *Pomc* expression (Fig. 7A)

and immunolabeling (Fig. 7B and C). Of note, the number and brightness of POMC+ melanotrophs and corticotrophs in double and triple mutant mice were normal (SI Appendix, Fig. S10) confirming that nPE1, nPE2, and nPE3 are hypothalamic *Pomc* enhancers that do not activate *Pomc* expression in the pituitary gland.

As a result of the very low levels of arcuate *Pomc* expression, Δ1Δ2/Δ1Δ2 and Δ1Δ2Δ3/Δ1Δ2Δ3 mice developed early-onset extreme obesity. The body weight growth curve of Δ1Δ2Δ3/Δ1Δ2Δ3 females peaked at a considerably steeper rate than in Δ1Δ2/Δ1Δ2 females (genotype vs. time effect,  $P < 0.05$  for Δ1Δ2 vs. Δ1Δ2Δ3, Fig. 8A), evidencing the relative contribution of nPE3 to *Pomc* expression levels and its impact in body weight homeostasis (Fig. 8A). By 16 wk of age Δ1Δ2Δ3/Δ1Δ2Δ3 females were ~10% heavier than Δ1Δ2/Δ1Δ2 females ( $49.8 \pm 1.0$  g vs.  $45.3 \pm 1.7$  g,  $P < 0.001$ , Fig. 8B). Both, Δ1Δ2/Δ1Δ2 and Δ1Δ2Δ3/Δ1Δ2Δ3 females displayed hyperphagia, consuming 43.1% and 52.2% more food per day, respectively, than their *wild-type* siblings (Fig. 8C and D). The significantly greater hyperphagia observed in triple mutant females was mainly due to increased food intake during the daylight period (9 am to 6 pm), a time in which the pattern of food consumption of Δ1Δ2/Δ1Δ2 females was normal (Fig. 8C). In addition, 16-wk-old Δ1Δ2Δ3/Δ1Δ2Δ3 females exhibited significantly longer nose-to-tail length ( $10.2 \pm 0.05$  cm vs.  $9.9 \pm 0.03$  cm,  $P = 0.01$ , Fig. 8E). Increased abdominal adiposity was also higher in Δ1Δ2Δ3/Δ1Δ2Δ3 than in Δ1Δ2/Δ1Δ2 females (Fig. 8F). This difference was apparent in visceral and gonadal white fat pads (Fig. 8G–J) and in interscapular brown fat (Fig. 8K). Interestingly, +/Δ1Δ2Δ3, but not +/Δ1Δ2, heterozygous females showed significantly heavier inguinal ( $P < 0.001$ ) and gonadal ( $P = 0.026$ ) white fat deposits compared to their control siblings (Fig. 8F–J). The livers of Δ1Δ2Δ3/Δ1Δ2Δ3 females were also heavier than in Δ1Δ2/Δ1Δ2 females (Fig. 8L). Finally, serum cholesterol, triglycerides, and blood glucose concentrations in triple and double homozygous mutants were higher than in *wild-type* siblings, and no differences were observed between Δ1Δ2Δ3/Δ1Δ2Δ3 and Δ1Δ2/Δ1Δ2 females in these parameters (Fig. 8M–O).

Different from what we observed between double and triple homozygous females, adult male mice lacking two or three hypothalamic *Pomc* enhancers displayed similar extreme obesity and body weight growth curves (Fig. 9A and B). However, Δ1Δ2Δ3/Δ1Δ2Δ3, but not Δ1Δ2/Δ1Δ2, males displayed greater hyperphagia during the daylight and lights-off periods relative to their respective *wild-type* controls, suggesting that nPE3 by itself is able to sustain some level of *Pomc* expression and contribute to the satiety tone exerted by central melanocortins (Fig. 9C and D). Most other metabolic parameters measured in double and triple homozygous males showed similar greater values in comparison to their *wild-type* siblings, with the exception of heavier inguinal fat deposits found in Δ1Δ2Δ3/Δ1Δ2Δ3 compared to Δ1Δ2/Δ1Δ2 males (Fig. 9H). All in all, our mutant mouse results demonstrate that nPE3 is a neuronal transcriptional enhancer which, together with nPE1 and nPE2, integrates a tripartite enhancer cluster that controls arcuate *Pomc* expression, food intake, and body weight.

## Discussion

When investigating the participation of the neuronal enhancers nPE1 and nPE2 in arcuate-specific *Pomc* expression using single and double enhancer mutant mice (12), we concluded that additional—yet unidentified—partially redundant enhancers were likely to participate in hypothalamic *Pomc* expression. Here, we followed a molecular evolution and genetics approach together with reporter expression analyses in transgenic zebrafish and mice that led us to the identification of nPE3, a neuronal *Pomc* enhancer

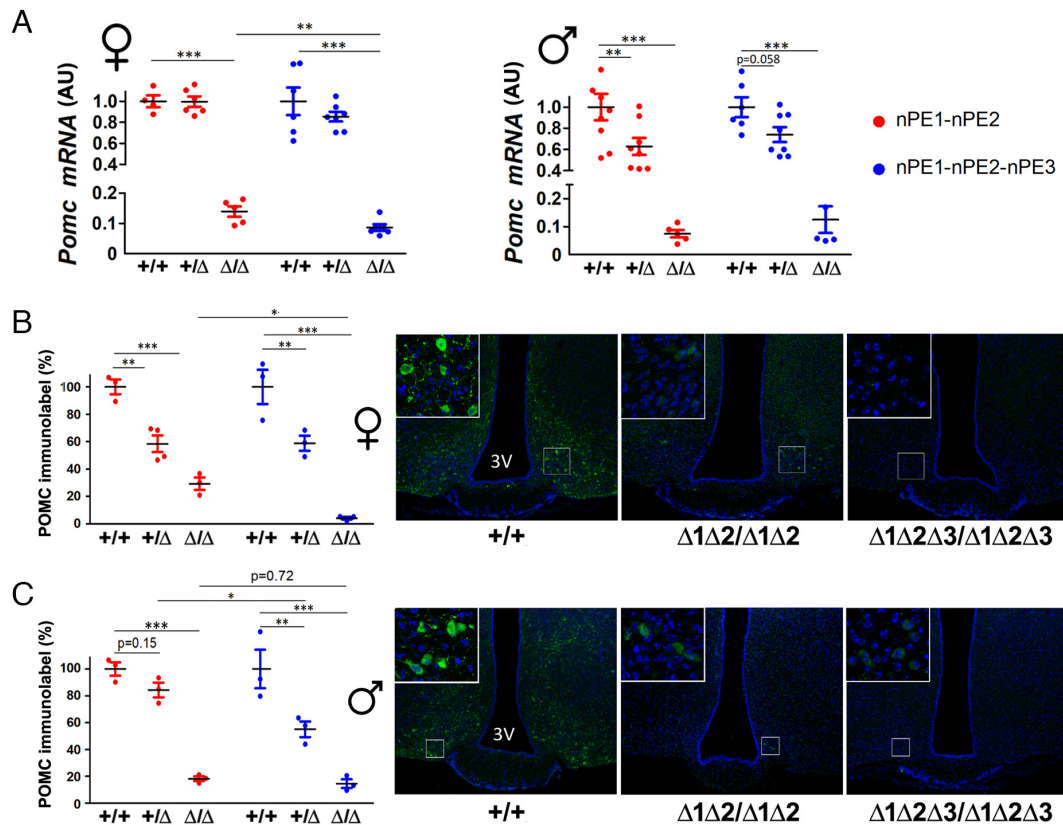


**Fig. 7.** Relative contribution of nPE3 to hypothalamic *Pomc* expression in adult mice. (A) qRT-PCR of *Pomc* mRNA obtained from hypothalami of *wild-type* (+/+), heterozygous *Pomc*<sup>+1Δ1Δ2</sup> or *Pomc*<sup>+1Δ1Δ2Δ3</sup> (+1Δ), and homozygous *Pomc*<sup>Δ1Δ2/Δ1Δ2</sup> or *Pomc*<sup>Δ1Δ2Δ3/Δ1Δ2Δ3</sup> (Δ1Δ) 16-wk-old females and males. *Pomc* mRNA was normalized to  $\beta$ -actin mRNA and expressed in AU. At least  $n = 4$  per group. (B and C, Left) Quantitative immunofluorescence using an anti-ACTH antibody in coronal brain sections of 16-wk-old females (B) and males (C) ( $n = 3$  to 5) represented as the product of the number of POMC+ cells and the mean integrated signal per cell in defined areas of three cryosections per mouse brain relative to +/+ same-sex littermates. (B and C, Right) Representative immunofluorescence in +/+, *Pomc*<sup>Δ1Δ2/Δ1Δ2</sup> (Δ1Δ2/Δ1Δ2), and *Pomc*<sup>Δ1Δ2Δ3/Δ1Δ2Δ3</sup> (Δ1Δ2Δ3/Δ1Δ2Δ3). Insets are confocal magnified views of the indicated boxes. 3V, third ventricle. Quantitative data represent the mean  $\pm$  SEM. Genotypes were compared by two-way ANOVA. \* $P < 0.05$ , \*\* $P < 0.01$ , \*\*\* $P < 0.001$ . Two-way ANOVA, followed by the Holm–Sidak post hoc test.

that is under purifying selection in all placental mammalian orders but absent in *Simiiformes* (monkeys, apes, and humans) due to a unique segmental deletion event. Targeted ablation of nPE3 from the mouse genome demonstrated that this regulatory element plays a fundamental role in the onset of *Pomc* expression in the developing ventromedial hypothalamus, as previously observed for nPE1 and nPE2 (12). In adult mice, nPE3 also contributes to neuronal *Pomc* expression by acting cooperatively with nPE1 and nPE2. In fact, nPE3 is the furthestmost 5' module of a *cis*-acting tripartite cluster of partially redundant enhancers that, together, fully control arcuate *Pomc* expression. This mammalian arcuate *POMC* enhancer cluster (*Mapec*) composed in a 5' to 3' orientation by nPE3, nPE1, and nPE2 is located in the 5' flanking region of the *POMC* locus of the vast majority of placental mammals (Fig. 3D), and maintains a relatively conserved distance to the *POMC* TSS (from 5.2 to 15 kb). *Mapec* spans a similar distance in all placental mammalian orders, being maximal in the sister groups Xenarthra and Afrotheria (~28 kb), and somewhat shorter in all other orders (4 to 17 kb), as if a segmental deletion had occurred between nPE3 and nPE1 in an ancestor to all members of the Boreoeutheria magnorder (Fig. 3D). *Mapec* adds to a still limited group of well-documented examples of partially redundant enhancer clusters, each of which controls the expression of genes such as *SOX2* (31), *MYC* (32), *FGF5* (33),  $\alpha$ -globin (33, 34), pancreas-associated TF 1A (*PTF1A*) (35), *Indian hedgehog homolog* (*IHH*) (36), and *SCN5A* (encoding the sodium channel NaV1.5) (37). Although the regulatory elements of these clusters are maintained under selective pressure, targeted deletions to the individual modules usually fail to produce deleterious phenotypes in mice.

This apparent contradiction unfolds when considering that clusters of partially redundant enhancers provide adaptive advantages such as increased transcriptional accuracy, expression levels, and robustness during environmental perturbations (38–41). In this regard, the adaptive value of having greater transcriptional efficiency of *POMC* in arcuate neurons is apparent. *POMC* encodes the anorexigenic melanocortins  $\alpha$ -,  $\beta$ -, and  $\gamma$ -MSH which are critical to maintain a satiety tone (1, 2), and the opioid peptide  $\beta$ -endorphin which induces stress-induced analgesia (42). Increased foraging exposes animals to unnecessary threats while hyperphagia and exaggerated adiposity are maladaptive in the wild because a greater body mass diminishes fertility and impairs survival skills in both, predator and prey (43). Likewise, robust  $\beta$ -endorphin-mediated analgesia is critical to sustain aggression, endurance, and long-lasting escapes in injured or wounded animals (44).

*Mapec* also shares typical features with *superenhancers* (45) including a great accumulation of TFBS contributed by the 3 nPEs which, jointly, are likely to gather multiple copies of several TFs that assure high-level expression of *POMC* in arcuate neurons. In *superenhancers*, such *cis-trans* molecular crowding of disordered C-terminal domains from multiple TFs, RNA polymerase II subunits, and many other cofactors stabilizes condensate-like structures in transcriptional hubs that activate gene expression at much higher levels than those achieved by “classical enhancers” (46–48). In this regard, *Pomc* is one of the earliest neuropeptide genes expressed in the mouse brain and among the highest expressed genes in the hypothalamus (2). Also, optimal *Pomc* expression has proven to be necessary to sustain normal levels of food intake in mice fed ad libitum (3, 12, 49).

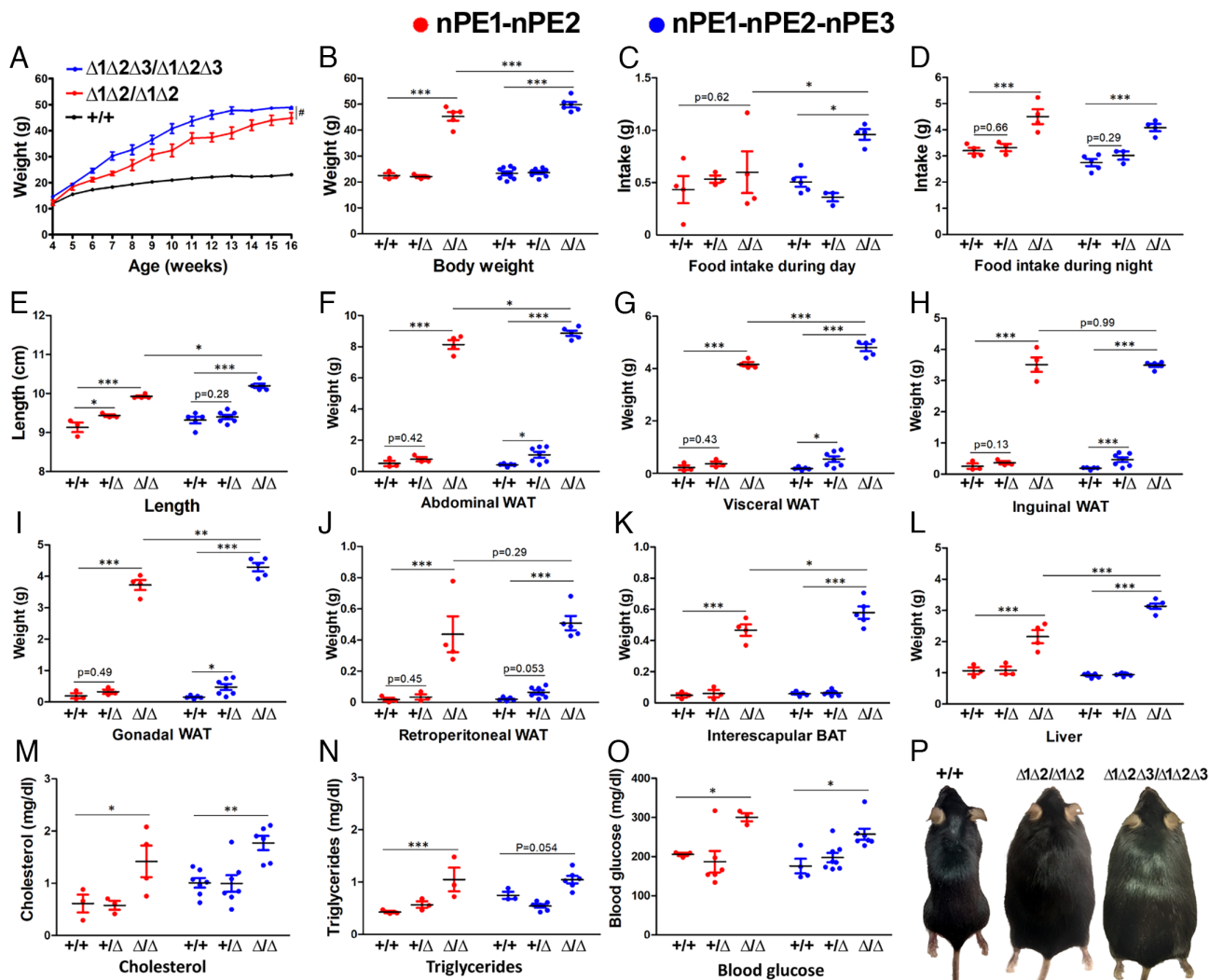


**Fig. 8.** Relative contribution of nPE3 to body weight homeostasis and metabolism in adult females. (A) Body weight curves of wild-type ( $+/+$ ), homozygous  $Pomc^{\Delta 1\Delta 2/\Delta 1\Delta 2}$  ( $\Delta 1\Delta 2/\Delta 1\Delta 2$ ) or  $Pomc^{\Delta 1\Delta 2\Delta 3/\Delta 1\Delta 2\Delta 3}$  ( $\Delta 1\Delta 2\Delta 3/\Delta 1\Delta 2\Delta 3$ ) females ( $n = 3$  to  $9$ ).  $\Delta 1\Delta 2\Delta 3/\Delta 1\Delta 2\Delta 3$  females display higher body weight compared to  $\Delta 1\Delta 2/\Delta 1\Delta 2$  females (RMA, genotype vs. time effect,  $\#P < 0.05$  for  $\Delta 1\Delta 2\Delta 3/\Delta 1\Delta 2\Delta 3$  vs.  $\Delta 1\Delta 2/\Delta 1\Delta 2$ ). (B–P) Metabolic phenotype of  $+/+$ ,  $Pomc^{\Delta 1\Delta 2/\Delta 1\Delta 2}$  or  $Pomc^{\Delta 1\Delta 2\Delta 3/\Delta 1\Delta 2\Delta 3}$  ( $\Delta 1\Delta 2$ ) and homozygous  $Pomc^{\Delta 1\Delta 2/\Delta 1\Delta 2}$  or  $Pomc^{\Delta 1\Delta 2\Delta 3/\Delta 1\Delta 2\Delta 3}$  ( $\Delta 1\Delta 2\Delta 3$ ) females at 16 wk of age. (B) Body weight ( $n = 3$  to  $9$ ). (C) Average food intake during the day time (9 am to 6 pm) and (D) during night time (6 pm to 9 am) measured over 5 consecutive days ( $n = 3$  to  $5$ ). (E) Nose-to-tail body length. (F–L) Determination of abdominal, visceral, inguinal, gonadal, and retroperitoneal white fat pads, interscapular brown fat pad weights, and liver weights ( $n = 3$  to  $7$ ). (M and N) Serum cholesterol and triglycerides concentration in females after an overnight fast (6 pm to 10 am) ( $n = 3$  to  $7$ ). (O) Blood glucose concentration after a 4 h fast (9 am to 1 pm) ( $n = 3$  to  $8$ ). Values represent mean  $\pm$  SEM.  $*P < 0.05$ ,  $**P < 0.01$ , and  $***P < 0.001$  (Two-way ANOVA). (P) Pictures of representative obese  $\Delta 1\Delta 2/\Delta 1\Delta 2$  and  $\Delta 1\Delta 2\Delta 3/\Delta 1\Delta 2\Delta 3$  females compared with a control sibling.

Another feature of *superenhancers* is the ability to recruit master TFs that dictate cell-specific identity at very early developmental stages and by being extremely vulnerable to local perturbations (45). In earlier studies, we have demonstrated that the master TF NKX2.1, essential to define the ventral identity of the developing hypothalamus, is also critical for the onset of hypothalamic *Pomc* expression and maintenance of POMC neurons' identity by binding to NKX canonical binding sites present in nPE1 and nPE2 (8), a result that we extend here for nPE3. Conditional *Nkx2.1* ablation from POMC neurons significantly reduced *Pomc* mRNA levels while increasing adiposity and body weight in adult mice (8). Perturbations in the *cis*-acting NKX binding sites of nPE1 and nPE2 also substantially impaired hypothalamic *Pomc* expression (8). In addition, selective ablation from POMC neurons of other TFs that participate in hypothalamic *Pomc* expression, such as ISL1, PRDM12, or TBX3, also showed drastic reductions in *Pomc* mRNA levels and invariably led to increased food intake and adiposity (7, 9, 10). All in all, our individual and multiple nPE deletion studies showing that the 3 nPEs act in a partially

redundant and cooperative manner [(12); and this paper] fit well with the idea that *Mapec* acts as a *superenhancer*.

That three unrelated sequences independently acquired over several million years the ability to activate *Pomc* expression in the same specific set of hypothalamic neurons is a formidable and intriguing example of triple convergent evolution of cell-specific transcriptional enhancer analogs. *Mapec* also constitutes a remarkable example of evolvability because the independent gathering of three functionally similar regulatory elements within a few kb upstream of a TSS generated an adaptive innovation capable of increasing transcriptional robustness for arcuate *Pomc* expression (50). The earliest neuronal *Pomc* mammalian enhancer nPE2 was fixed in the *POMC* locus sometime after the origin of egg-laying mammals (~200 mya) and before the Prototheria/Metatheria split (170 to 190 mya) (15–17) following the exaptation of a CORE-SINE retroposon (13). Whether nPE2 acts as a single “classical” arcuate *POMC* enhancer in monotremes and marsupials is a matter of speculation. A possible scenario to envision *Mapec*'s origin is that after the Metatheria/Eutheria split (~160 mya) and

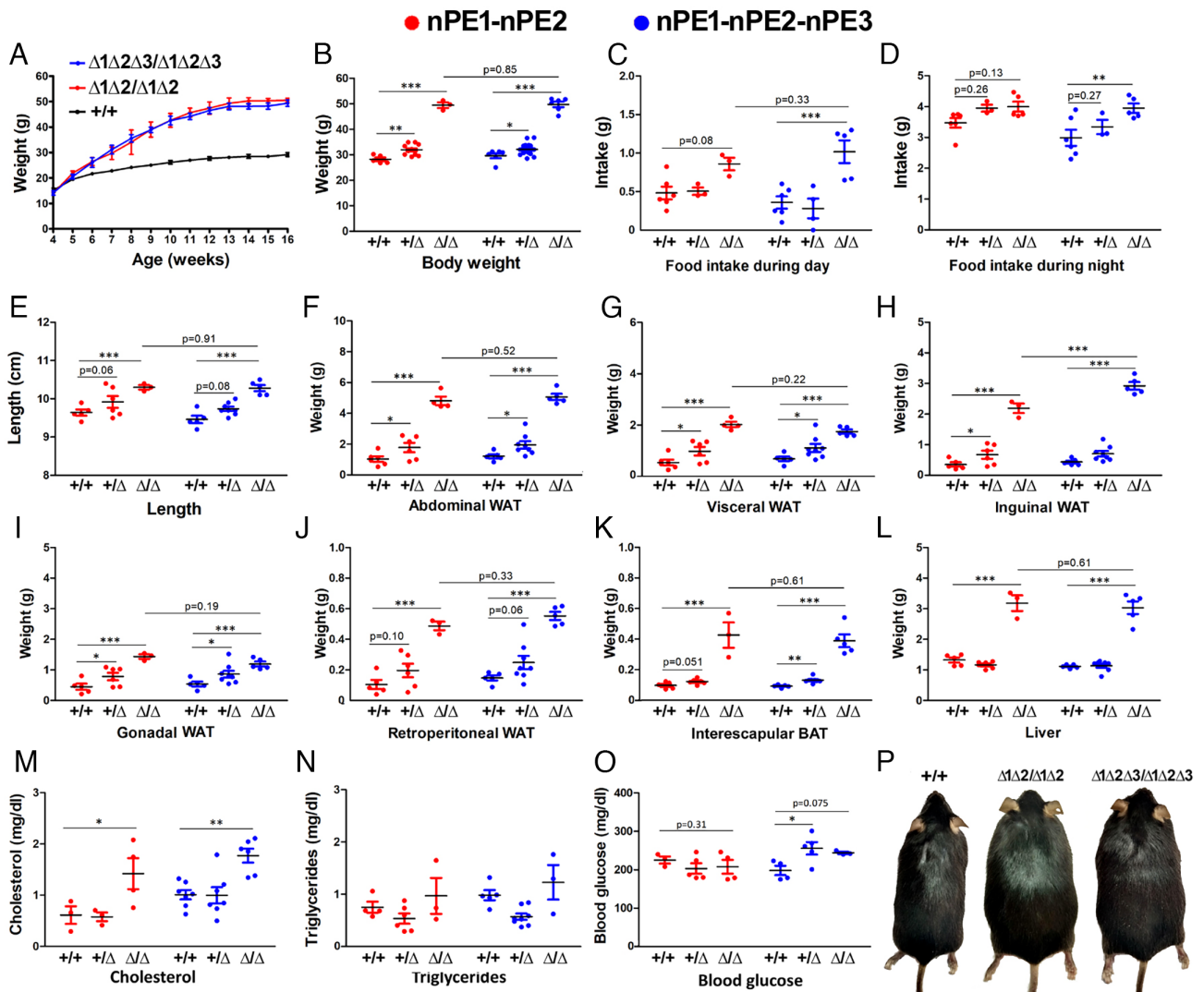


**Fig. 9.** Relative contribution of nPE3 to body weight homeostasis and metabolism in adult males. (A) Body weight curves of *wild-type* ( $+/+$ ), homozygous *Pomc* <sup>$\Delta 1\Delta 2/\Delta 1\Delta 2$</sup>  ( $\Delta 1\Delta 2/\Delta 1\Delta 2$ ) or *Pomc* <sup>$\Delta 1\Delta 2\Delta 3/\Delta 1\Delta 2\Delta 3$</sup>  ( $\Delta 1\Delta 2\Delta 3/\Delta 1\Delta 2\Delta 3$ ) males (n = 3 to 16). (B–P) Metabolic phenotype of  $+/+$ , *Pomc* <sup>$\Delta 1\Delta 2$</sup>  or *Pomc* <sup>$\Delta 1\Delta 2\Delta 3$</sup>  ( $+/\Delta$ ), and homozygous *Pomc* <sup>$\Delta 1\Delta 2/\Delta 1\Delta 2$</sup>  or *Pomc* <sup>$\Delta 1\Delta 2\Delta 3/\Delta 1\Delta 2\Delta 3$</sup>  ( $\Delta/\Delta$ ) males at 16 wk of age. (B) Body weight (n = 3 to 16). (C) Average food intake during the day time (9 am to 6 pm) and (D) during night time (6 pm to 9 am) measured over 5 consecutive days (n = 3 to 6). (E) Nose-to-tail body length. (F–L) Determination of abdominal, visceral, inguinal, gonadal, and retroperitoneal white fat pads, interscapular brown fat pad weights, and liver weights (n = 3 to 7). (M and N) Serum cholesterol and triglycerides concentration in males after an overnight fast (6 pm to 10 am) (n = 3 to 7). (O) Blood glucose concentration after a 4 h fast (9 am to 1 pm) (n = 3 to 5). Values represent mean  $\pm$  SEM. \**P* < 0.05, \*\**P* < 0.01, and \*\*\**P* < 0.001 (Two-way ANOVA). (P) Pictures of representative obese  $\Delta 1\Delta 2/\Delta 1\Delta 2$  and  $\Delta 1\Delta 2\Delta 3/\Delta 1\Delta 2\Delta 3$  males compared with a control sibling.

before the radiation of placental mammals (~100 mya) ancient TE-derived dormant sequences upstream of nPE2 acquired a series of mutations that created combinations of TFBS compatible with TFs involved in arcuate-specific *POMC* expression, leading to the sequential and independent origins of nPE1 and nPE3 (or vice versa). Once these placental novelties earned adaptive value they started to evolve under purifying selection and, together with nPE2, assembled *Mapec*, a tripartite syntenic enhancer cluster with strengthened capacity for *Pomc* expression and regulation present in all placental mammalian orders.

The *cis*-acting regulatory elements controlling neuronal *POMC* expression underwent several episodes of enhancer turnover throughout vertebrate evolution, as we reported when comparing lineage-specific hypothalamic *POMC* expression strategies among members of the teleost superorders Ostariophysi (zebrafish) and Acanthopterygii (tetraodon, fugu, stickleback and medaka) with placental and nonplacental mammals (21). During those studies, we found that mouse nPE1 and nPE2 were able to drive reporter gene expression specifically to hypothalamic *POMC* neurons in

transgenic zebrafish, indicating that despite complete enhancer turnover the *cis-trans* code of neuronal *POMC* expression has been conserved since the divergence of the teleost and tetrapod lineages, more than 450 mya (21). Moreover, we showed that *ISL1* coexpresses with *POMC* in ventral hypothalamic neurons of mice and zebrafish, and also that both *ISL1* orthologs are critical for the onset of *POMC* expression in each of these distant vertebrate species (7). Enhancer mutations and turnover are main drivers of variation, innovation, and animal diversity during evolution (51), as has been originally suggested (52). In particular, loss of cell-specific enhancers may lead to drastic phenotypic changes, as documented in notorious examples. For example, formation of the pelvic bony spines in three-spined sticklebacks depends on the presence of a specific pelvic enhancer driving *Pitx1* expression to the pelvic region of these teleost fishes (53). This enhancer is present in spiny sticklebacks that live in the sea where they can be better protected from marine predators. In contrast, several freshwater stickleback populations lacking pelvic spines are associated with deletions in the *Pitx1* pelvic enhancer, which are likely the consequence of a looser

selective pressure in a safer environment (53). Another stunning example has been more recently reported in several snake genomes which carry loss of function mutations in a long-distance enhancer of *Shh* that is essential for limb formation in vertebrates (53, 54). In humans, a study identified a noncoding region in the androgen receptor (AR) locus which is highly conserved in all mammals but absent from the human genome. When this mouse or chimpanzee element was tested in transgenic mice, it proved to be an enhancer driving reporter gene expression to vibrissae (sensory hairs in the face) and the genital tubercle (55). Thus, the loss of this enhancer in the lineage leading to humans may explain why sensory facial vibrissae and penile spines are present in rodents and nonhuman primates but absent in our species (55). Here, we report that nPE3 was lost in the lineage leading to Simiiformes (Anthropoids), a primate infraorder that includes Platyrrhini (New World monkeys) and Catarrhini (Old World monkey, gibbons, great apes, and humans). Different from other cases of loss of enhancer function caused by deleterious mutations in critical TFBS (53, 54), the absence of nPE3 is possibly due to a ~10 kb lineage-specific segmental deletion that occurred in an ancestor to all Simiiformes sometime after the Tarsiiformes/Simiiformes split (~62 mya) and before the divergence of Platyrrhini and Catarrhini (~39 mya). Because the tripartite enhancer cluster *Mapec* has been under strong purifying selection since its origin and for the last 100 million years in all placental mammalian orders, the segmental deletion that occurred in a Simiiformes ancestor is likely to have been fixed in the population by genetic drift at a time and place in primate history that did not induce considerable maladaptive consequences (neutral or near neutral effects). From a physiological perspective, our nPE3 mutants may be viewed as a *simiiformized* mouse model of transcriptional control of hypothalamic *Pomc* expression in which the deletion of one of the partially redundant modules of *Mapec* seems to be mostly compensated by the others, at least in mice living in the standardized and almost invariable conditions of a modern mouse facility. However, we cannot rule out the possibility that the loss of nPE3 was selected during particular environmental circumstances in which elevated food intake and reduced energy expenditure increased fitness. Based on the rich history of neuronal *Pomc* enhancer turnover along vertebrate evolution (21), it is also tempting to speculate that this process continued in Simiiformes giving rise to modified versions of *Mapec*. Whether novel neuronal *Pomc* enhancers integrate *Mapec* in Humans remains to be explored. Finally, our study highlights the importance to evaluate the individual modular contribution and emergent properties of partially redundant enhancer clusters by inactivating each element from their native genomic locus in a comprehensive

series of mutant mice where to compare not only the effect of each mutation in gene expression but also the physiological consequences and fitness of the individual mutants in both sexes and at different embryonic and postnatal ages.

## Materials and Methods

**Sequence Analysis and Databases.** Reference human genome hg19 (GRCh37) and mouse genome mm9 (NCBI37) and mm10 (GRCm38) were used. Functional genomics data were obtained from the ENCODE project (<https://www.encodeproject.org>) (56). More details are provided in *SI Appendix, Supplementary Materials and Methods*.

**Animal Care.** Zebrafish experiments were performed in *wild-type* AB strain from the Zebrafish International Resource Center from the University of Oregon. Adult zebrafish were maintained at 28 °C in a 14/10 h light/dark cycle in a completely automatic aquarium (Aquatic Habitats). Mice were housed in ventilated cages under controlled temperature and photoperiod (12-h light/12-h dark cycle, lights on from 7:00 AM to 7:00 PM), with tap water and laboratory chow containing 28.8% protein, 5.33% fat, and 65.87% carbohydrate available ad libitum. All animal procedures followed the Guide for the Care and Use of Laboratory Animals (57) and in agreement with the Institutional Animal Care and Use Committee of the Instituto de Investigaciones en Ingeniería Genética y Biología Molecular (INGEBI, CONICET). More details for the transcription enhancer assay in zebrafish, transgenic and mutant mice production, and experimental analysis are provided in *SI Appendix, Supplementary Materials and Methods*.

**Data, Materials, and Software Availability.** Transgenic zebrafish, mice, and plasmids are available upon request. All data necessary for confirming the conclusions of the article are present within the article, figures, and tables. All databases and software used are public and properly named and indicated in the *Results* and *Materials and Methods*. All other data are included in the manuscript and/or *supporting information*.

**ACKNOWLEDGMENTS.** We thank Marta Treimun and Dante Montini for valuable technical assistance. This work was supported by NIH Grant R01 DK068400 (to M.J.L. and M.R.) and PICT (Proyectos de Investigación Científicos y Tecnológicos) grants from the Agencia Nacional de Promoción Científica y Tecnológica, Argentina (M.R.). D.R., C.E.H., and A.S. were recipients of doctoral fellowships from CONICET (Consejo Nacional de Investigaciones Científicas y Técnicas), Argentina.

Author affiliations: <sup>a</sup>Instituto de Investigaciones en Ingeniería Genética y Biología Molecular, Consejo Nacional de Investigaciones Científicas y Técnicas, Buenos Aires 1428, Argentina; <sup>b</sup>Departamento de Fisiología, Biología Molecular y Celular, Facultad de Ciencias Exactas y Naturales, Universidad de Buenos Aires, Buenos Aires 1428, Argentina; <sup>c</sup>Instituto de Fisiología, Biología Molecular y Neurociencias, Universidad de Buenos Aires and Consejo Nacional de Investigaciones Científicas y Técnicas, Buenos Aires 1428, Argentina; and <sup>d</sup>Department of Molecular and Integrative Physiology, University of Michigan, Ann Arbor, MI 48105

- J. C. Brüning, H. Fenselau, Integrative neurocircuits that control metabolism and food intake. *Science* **381**, eabl7398 (2023).
- M. Rubinstein, M. J. Low, Molecular and functional genetics of the proopiomelanocortin gene, food intake regulation and obesity. *FEBS Lett.* **591**, 2593–2606 (2017).
- V. F. Bumacshny *et al.*, Obesity-programmed mice are rescued by early genetic intervention. *J. Clin. Invest.* **122**, 4203–4212 (2012).
- H. Krude *et al.*, Severe early-onset obesity, adrenal insufficiency and red hair pigmentation caused by POMC mutations in humans. *Nat. Genet.* **19**, 155–157 (1998).
- L. Yaswen, N. Diehl, M. B. Brennan, U. Hochgeschwender, Obesity in the mouse model of pro-opiomelanocortin deficiency responds to peripheral melanocortin. *Nat. Med.* **5**, 1066–1070 (1999).
- E. Raffan *et al.*, A deletion in the canine POMC gene is associated with weight and appetite in obesity-prone labrador retriever dogs. *Cell Metab.* **23**, 893–900 (2016).
- S. Nasif *et al.*, Islet 1 specifies the identity of hypothalamic melanocortin neurons and is critical for normal food intake and adiposity in adulthood. *Proc. Natl. Acad. Sci. U.S.A.* **112**, E1861–E1870 (2015).
- D. P. Orquera *et al.*, The homeodomain transcription factor NKX2.1 is essential for the early specification of melanocortin neuron identity and activates expression in the developing hypothalamus. *J. Neurosci.* **39**, 4023–4035 (2019).
- C. E. Hael, D. Rojo, D. P. Orquera, M. J. Low, M. Rubinstein, The transcriptional regulator PRDM12 is critical for *Pomc* expression in the mouse hypothalamus and controlling food intake, adiposity, and body weight. *Mol. Metab.* **34**, 43–53 (2020).
- C. Quarta *et al.*, Functional identity of hypothalamic melanocortin neurons depends on Tbx3. *Nat. Metab.* **1**, 222–235 (2019).
- F. S. J. de Souza *et al.*, Identification of neuronal enhancers of the proopiomelanocortin gene by transgenic mouse analysis and phylogenetic footprinting. *Mol. Cell. Biol.* **25**, 3076–3086 (2005).
- D. D. Lam *et al.*, Partially redundant enhancers cooperatively maintain mammalian *Pomc* expression above a critical functional threshold. *PLoS Genet.* **11**, e1004935 (2015).
- A. M. Santangelo *et al.*, Ancient exaptation of a CORE-SINE retroposon into a highly conserved mammalian neuronal enhancer of the proopiomelanocortin gene. *PLoS Genet.* **3**, 1813–1826 (2007).
- L. F. Franchini *et al.*, Convergent evolution of two mammalian neuronal enhancers by sequential exaptation of unrelated retroposons. *Proc. Natl. Acad. Sci. U.S.A.* **108**, 15270–15275 (2011).
- O. R. P. Bininda-Emonds *et al.*, The delayed rise of present-day mammals. *Nature* **446**, 507–512 (2007).
- N. M. Foley *et al.*, A genomic timescale for placental mammal evolution. *Science* **380**, eabl8189 (2023).
- M. J. Christmas *et al.*, Evolutionary constraint and innovation across hundreds of placental mammals. *Science* **380**, eabn3943 (2023).
- A. Siepel *et al.*, Evolutionarily conserved elements in vertebrate, insect, worm, and yeast genomes. *Genome Res.* **15**, 1034–1050 (2005).
- M. Blanchette *et al.*, Aligning multiple genomic sequences with the threaded blockset aligner. *Genome Res.* **14**, 708–715 (2004).
- W. J. Kent, BLAT: The BLAST-like alignment tool. *Genome Res.* **12**, 656–664 (2002).
- S. Domené *et al.*, Enhancer turnover and conserved regulatory function in vertebrate evolution. *Philos. Trans. R. Soc. Lond. B, Biol. Sci.* **368**, 20130027 (2013).

22. S. F. Altschul, W. Gish, W. Miller, E. W. Myers, D. J. Lipman, Basic local alignment search tool. *J. Mol. Biol.* **215**, 403–410 (1990).
23. M. A. Larkin *et al.*, Clustal W and Clustal X version 2.0. *Bioinformatics* **23**, 2947–2948 (2007).
24. T. A. Tatusova, T. L. Madden, BLAST 2 Sequences, a new tool for comparing protein and nucleotide sequences. *FEMS Microbiol. Lett.* **174**, 247–250 (1999).
25. L. Elnitski, R. Burhans, C. Riemer, R. Hardison, W. Miller, MultiPipMaker: A comparative alignment server for multiple DNA sequences. *Curr. Protoc. Bioinf.* **10**, 10.4.1–10.4.14 (2010).
26. Y. Shao *et al.*, Phylogenomic analyses provide insights into primate evolution. *Science* **380**, 913–924 (2023).
27. J. A. Castro-Mondragon *et al.*, JASPAR 2022: The 9th release of the open-access database of transcription factor binding profiles. *Nucl. Acids Res.* **50**, D165–D173 (2022).
28. F. S. J. de Souza *et al.*, The estrogen receptor  $\alpha$  colocalizes with proopiomelanocortin in hypothalamic neurons and binds to a conserved motif present in the neuron-specific enhancer nPE2. *Eur. J. Pharmacol.* **660**, 181–187 (2011).
29. H. Yu, M. Rubinstein, M. J. Low, Developmental single-cell transcriptomics of hypothalamic POMC neurons reveal the genetic trajectories of multiple neuropeptidergic phenotypes. *eLife* **11**, e22883 (2022).
30. S. L. Padilla, J. S. Carmody, L. M. Zeltser, Pomc-expressing progenitors give rise to antagonistic neuronal populations in hypothalamic feeding circuits. *Nat. Med.* **16**, 403–405 (2010).
31. H. Y. Zhou *et al.*, A Sox2 distal enhancer cluster regulates embryonic stem cell differentiation potential. *Genes Dev.* **28**, 2699–2711 (2014).
32. C. Bahr *et al.*, A Myc enhancer cluster regulates normal and leukaemic haematopoietic stem cell hierarchies. *Nature* **553**, 515–520 (2018).
33. H. F. Thomas *et al.*, Temporal dissection of an enhancer cluster reveals distinct temporal and functional contributions of individual elements. *Mol. Cell* **81**, 969–982.e13 (2021).
34. M. Kassouf, S. Ford, J. Blayney, D. Higgs, Understanding fundamental principles of enhancer biology at a model locus: Analysing the structure and function of an enhancer cluster at the  $\alpha$ -globin locus. *Bioessays* **45**, e2300047 (2023).
35. I. Miguel-Escalada *et al.*, Pancreas agenesis mutations disrupt a lead enhancer controlling a developmental enhancer cluster. *Dev. Cell* **57**, 1922–1936.e9 (2022).
36. A. J. Will *et al.*, Composition and dosage of a multipartite enhancer cluster control developmental expression of IHH (Indian hedgehog). *Nat. Genet.* **49**, 1539–1545 (2017).
37. J. C. K. Man *et al.*, An enhancer cluster controls gene activity and topology of the SCN5A-SCN10A locus in vivo. *Nat. Commun.* **10**, 4943 (2019).
38. T. Montavon *et al.*, A regulatory archipelago controls Hox genes transcription in digits. *Cell* **147**, 1132–1145 (2011).
39. C. P. Fulco *et al.*, Systematic mapping of functional enhancer–promoter connections with CRISPR interference. *Science* **354**, 769–773 (2016).
40. M. Osterwalder *et al.*, Enhancer redundancy provides phenotypic robustness in mammalian development. *Nature* **554**, 239–243 (2018).
41. F. Grosveld, J. van Staalduinen, R. Stadhouders, Transcriptional regulation by (super)enhancers: From discovery to mechanisms. *Annu. Rev. Genomics Hum. Genet.* **22**, 127–146 (2021).
42. M. Rubinstein *et al.*, Absence of opioid stress-induced analgesia in mice lacking beta-endorphin by site-directed mutagenesis. *Proc. Natl. Acad. Sci. U.S.A.* **93**, 3995–4000 (1996).
43. J. R. Speakman, Evolutionary perspectives on the obesity epidemic: Adaptive, maladaptive, and neutral viewpoints. *Annu. Rev. Nutr.* **33**, 289–317 (2013).
44. R. J. Bodnar, Endogenous opiates and behavior: 2022. *Peptides* **169**, 171095 (2023).
45. W. A. Whyte *et al.*, Master transcription factors and mediator establish super-enhancers at key cell identity genes. *Cell* **153**, 307–319 (2013).
46. B. R. Sabari *et al.*, Coactivator condensation at super-enhancers links phase separation and gene control. *Science* **361**, eaar3958 (2018).
47. D. Hnisz, K. Shrinivas, R. A. Young, A. K. Chakraborty, P. A. Sharp, A phase separation model for transcriptional control. *Cell* **169**, 13–23 (2017).
48. S. Hahn, Phase separation, protein disorder, and enhancer function. *Cell* **175**, 1723–1725 (2018).
49. K. H. Chhabra *et al.*, Reprogramming the body weight set point by a reciprocal interaction of hypothalamic leptin sensitivity and Pomc gene expression reverts extreme obesity. *Mol. Metab.* **5**, 869–881 (2016).
50. A. Wagner, Robustness and evolvability: A paradox resolved. *Proc. Biol. Sci.* **275**, 91–100 (2008).
51. M. Rubinstein, F. S. J. de Souza, Evolution of transcriptional enhancers and animal diversity. *Philos. Trans. R. Soc. Lond. B, Biol. Sci.* **368**, 20130017 (2013).
52. M. C. King, A. C. Wilson, Evolution at two levels in humans and chimpanzees. *Science* **188**, 107–116 (1975).
53. Y. F. Chan *et al.*, Adaptive evolution of pelvic reduction in sticklebacks by recurrent deletion of a Pitx1 enhancer. *Science* **327**, 302–305 (2010).
54. E. Z. Kvon *et al.*, Progressive loss of function in a limb enhancer during snake evolution. *Cell* **167**, 633–642.e11 (2016).
55. C. Y. McLean *et al.*, Human-specific loss of regulatory DNA and the evolution of human-specific traits. *Nature* **471**, 216–219 (2011).
56. ENCODE Project Consortium *et al.*, Expanded encyclopaedias of DNA elements in the human and mouse genomes. *Nature* **583**, 699–710 (2020).
57. National Research Council, Division on Earth and Life Studies, Institute for Laboratory Animal Research, Committee for the Update of the Guide for the Care and Use of Laboratory Animals, *Guide for the Care and Use of Laboratory Animals: Eighth Edition* (National Academies Press, 2010).